Microscopic Structure of Amorphous Covalent Alloys Probed by *Ab Initio* Molecular Dynamics: SiC

Fabio Finocchi,(1),(a) Giulia Galli,(2),(b) Michele Parrinello,(2) and Carlo M. Bertoni(1)
(1)*Dipartimento di Fisica, II Università di Roma "Tor Vergata," Via E. Carnevale, I-00173 Roma, Italy*
(2)*IBM Research Division, Zurich Research Laboratory, 8803 Rüschlikon, Switzerland*

(Received 25 February 1992)

We performed *ab initio* molecular-dynamics simulations of an equimolar Si-C amorphous alloy. *a*-SiC is found not to exhibit chemical order and to be much more complex than commonly believed. Our simulation is in good agreement with most measurements, although many interpretations of experimental data disagree with our results. The reasons for this discrepancy are analyzed and it is proposed that neutron scattering experiments can resolve the issue. Our study highlights the importance of reliable techniques complementary to experiment for a full characterization of amorphous semiconducting alloys.

PACS numbers: 61.42.+h, 61.55.Hg, 71.20.Cf

Amorphous semiconducting alloys (ASA) are of both fundamental and technological interest [1,2]. The fundamental interest is in the modification of chemical ordering, types of bonds, and coordination between the different atomic species, with respect to the corresponding crystals. The technological interest arises from the high-temperature stability of their semiconducting properties, which make ASA potentially useful as semiconductors in or close to engines, turbines, and reactors. Furthermore, the optical and electronic characteristics of many ASA suggest potential uses for the technology of solar cells, photovoltaic devices, and refractory materials.

In the past few decades, diffraction and spectroscopic measurements have provided valuable information about both structural and electronic properties of several disordered semiconducting alloys. However, because of difficulties in obtaining detailed information about *each* atomic species the interpretation of experiments is rather controversial and a complete characterization of these materials has not yet been achieved. On the other hand, the complexity of the chemical bond in covalent disordered alloys and the difficulties of accounting for quantum effects relevant to its correct description have limited most theoretical investigations to modeling experimental data; only recently have computer simulations with empirical potentials [3] and tight-binding (TB) calculations [4] appeared in the literature.

Of particular interest and complexity are the materials like *a*-SiC, composed of species whose chemical behavior is radically different. It is well known that C is capable of different hybrids (sp, sp^2, and sp^3) giving rise to crystals and disordered solids with a great diversity of properties, whereas Si usually prefers fourfold sp^3 coordination at low temperature and pressure. Key questions about *a*-SiC are yet unanswered, e.g., the ratio of homonuclear to heteronuclear bonds, the kind of coordination disorder, and the bonds formed by C atoms. Two lines of thought have emerged from the interpretation of different experiments. Some authors describe *a*-SiC as not chemically ordered, with both homonuclear and heteronuclear bonds. Others characterize the system as highly ordered, with predominantly Si-C bonds, as found in the corresponding crystal. In particular, Gorman and Solin [5] interpreted their Raman spectra on sputtered *a*-$Si_{0.59}C_{0.41}$ as direct evidence of homonuclear bonds and of the existence of both graphitelike and diamondlike C sites. This is consistent with the analysis of valence-band spectra by Fang and Ley [6] and with the x-ray diffraction (XRD) data of Tejeda, Shevchik, and Cardona [7]. The x-ray photoemission spectroscopy and Auger spectra by Lee [8] are interpreted as evidence of chemical order. However, also a small amount of Si-Si and C-C bonds are detected in their samples. Similar conclusions are drawn in Refs. [9,10], which present the analysis of extended x-ray-absorption fine-structure (EXAFS) spectra and XRD data. From the total correlation function of *a*-Si_xC_{1-x} ($x \simeq 0.5$) derived from electron diffraction data, whose peaks are positioned close to the neighbor distances in *c*-SiC, Sproul, McKenzie, and Cockayne [11] deduce that the system is composed of a tetrahedral network which is predominately heteronuclear bonded. Also Kaloyeros, Rizk, and Woodhouse [12] characterize *a*-SiC as chemically ordered, since the peak positions of Fourier transformed (FT) intensities obtained in electron energy loss measurements are close to the corresponding ones in *c*-SiC. This picture is in apparent disagreement with very recent electron spin resonance experiments [13], which show the presence of sp^2 carbon in *a*-SiC, constituting polymerlike networks with C=C bonds.

In order to resolve these issues, we have performed first-principles [14] molecular-dynamics (MD) simulations of *a*-$Si_{0.5}$:$C_{0.5}$. Quantum interactions between atoms are described by density functional theory in the local density approximation. *Ab initio* MD has proven to be very successful in predicting a variety of properties of disordered systems, among them *a*-C [15] and *a*-Si [16]. We find that *a*-SiC has a more complex structure than previously understood. Our data are in agreement with most of the existing experiments, although in apparent disagreement with the interpretation of several of them, and show that a detailed analysis of each atomic species (e.g., of *partial* as opposed to *total* distribution functions) is crucial to the understanding of the material properties. Indeed, we find that different structural models implying different kinds of chemical bonds and coordination disorder can be compatible with the same set of measurements. This is expected to be the case for the whole family of ASA and highlights the importance of reliable techniques complementary to experiment for a full characterization of their microscopic structure.

In our calculations, *a*-SiC networks at stoichiometric composition and room temperature were obtained by quenching from a liquid. We have carried out MD simulations for 54 and 64 atoms. Only the Γ point of the MD supercell Brillouin zone (BZ) has been sampled. In an ordered crystal this would correspond to different samplings of the primitive cell BZ. The macroscopic density (ρ_0) has been fixed at the experimental density of *c*-SiC [17]. The single-particle electronic orbitals have been expanded in plane waves, with a maximum kinetic energy (E_{cut}) of 35 Ry. For the expansion of the charge density and potential, $E_{\mathrm{cut}}=140$ Ry was used. The interaction between valence and core electrons has been described by *ab initio* nonlocal pseudopotentials [18,19]. In order to ensure that the properties of the liquid and hence of the amorphous networks generated in our simulation are not biased by the initial configuration chosen, we generated two liquidlike states starting from completely different initial conditions. In one (the 54-atom sample) the atoms of the two species occupy the diamond crystal positions randomly, thus also allowing homonuclear bonds. In the other (the 64-atom sample) they are arranged in the rocksalt structure, where only heteronuclear bonds are present. Both samples were heated to $T\simeq 4000$ K, where the system shows a diffusive behavior and is therefore characterized as a liquid, equilibrated for about 1 ps and then cooled to $T\simeq 500$ K [20]. The structural and bonding properties of the two networks thus generated are very similar. We therefore conclude that the model of *a*-SiC obtained in our simulation is not affected by the initial conditions chosen, not by different k points sampling of the BZ. In the following we describe our data for the 54-atom sample. Detailed analysis of both samples will be reported elsewhere.

Figure 1 displays the computed partial distribution functions (PDF) $g_{i\text{-}j}$ $(i,j=\mathrm{C,Si})$. The $g_{\mathrm{C\text{-}C}}$ curve has an intense first peak at 1.50 Å, to be compared with the nearest-neighbor distances (d_{nn}) calculated [15] for graphite (1.43 Å) and diamond (1.55 Å). The partial coordination number of C $(n_{\mathrm{C\text{-}C}})$, as computed from the integral of $g_{\mathrm{C\text{-}C}}$ up to its first minimum at 2 Å, is about 1.8. The $g_{\mathrm{C\text{-}C}}$ curve has two secondary maxima at 2.51 and 2.94 Å. The first is the most intense one, close to the next-nearest-neighbor distance in diamond (2.49 Å), and corresponds to carbons both bonded to a like atom (C-C-C configuration), whereas the second peak corresponds to C-Si-C configurations. C atoms are found to form both sp^2 and sp^3 sites, in agreement with experimental evidence [7,21–23], and consistent with the results of recent Monte Carlo simulations [3]. In particular, in our samples 15% of the C sites are coordinated threefold, with preferred bond angles close to 120°. The partial angular distributions of threefold and fourfold C atoms have maxima close to the graphitic and tetrahedral angles, respectively.

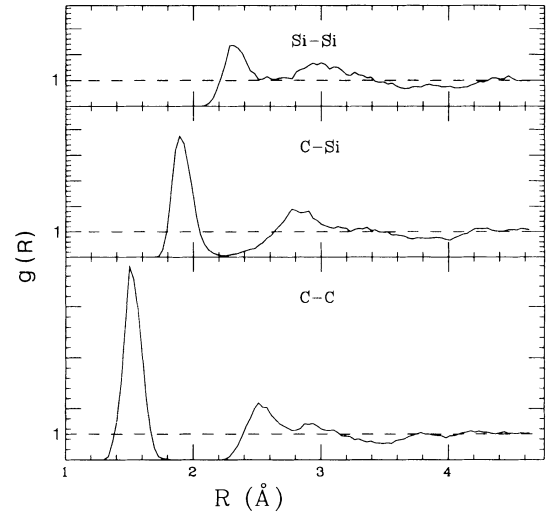

FIG. 1. Computed radial distribution functions $g_{i\text{-}j}$, $i,j=\mathrm{C,Si}$.

The first maximum of $g_{\mathrm{Si\text{-}C}}$ (Fig. 1) is at 1.89 Å, which corresponds to the computed d_{nn} in *c*-SiC. The value of $n_{\mathrm{Si\text{-}C}}$ is calculated to be $\simeq 2.1$; this, together with the result for $n_{\mathrm{C\text{-}C}}$, gives a total C coordination smaller than 4.0. The $g_{\mathrm{Si\text{-}C}}$ curve has a pronounced secondary peak at 2.85 Å, followed by a shoulder at about 3.4 Å. As is the case for the secondary maxima of $g_{\mathrm{C\text{-}C}}$, these structures are related to different bonding arrangements of the two species, in particular to C-C-Si and C-Si-Si configurations. $g_{\mathrm{Si\text{-}Si}}$ is less structured than the other PDF. It has a first maximum at a distance close to d_{nn} in diamond Si (2.32 Å) and a broad secondary peak spread over 0.6 Å. Its first minimum is not well defined, making the definition of $n_{\mathrm{Si\text{-}Si}}$ distance dependent [24]. These results together with those obtained for the angular distribution of Si atoms, which has a broad peak around 105°, an angle smaller than the tetrahedral angle (109°), indicates that the network formed by Si sites is a distorted tetrahedral network, more disordered than the one found, e.g., in *a*-Si [16].

The picture of *a*-SiC which emerges from our structural analysis is rather complex: (40–45)% of the bonds formed by C are homonuclear, quite unlike the structure of *c*-SiC. C atoms, which give rise to both sp^2 and sp^3 sites, tend to form chainlike structures, surrounded by Si-C and Si-Si networks, where Si give rise to strongly distorted diamondlike sites. These findings, which are consistent with recent TB calculations [4], are in apparent disagreement with the interpretation of several experimental data. In order to understand this discrepancy, it is useful to compare directly our results with XRD data. From the computed partial structure factors (SF) $S_{i,j}(\mathbf{q}) = \langle \sum_{i,j} \exp(-i\mathbf{q}\cdot\mathbf{R}_i)\exp(-i\mathbf{q}\cdot\mathbf{R}_j)\rangle$ (where $\mathbf{R}$ are atomic positions and $\langle\,\rangle$ denote averages taken over 1 ps at $T \simeq 500$ K), we can construct the total distribution function $j_{\mathrm{XR}}(r)$ [Fig. 2(a)] to be compared with the Fourier transform of measured scattered intensities. We have obtained $j_{\mathrm{XR}}(r)$ as the FT of the total SF [25],

$$S(q) = \frac{\sum_{i,j} f_i(q) f_j(q) S_{i,j}(q)}{\sum_i f_i(q)^2}, \tag{1}$$

where $f_i(q)$ are x-ray atomic scattering factors from Ref. [26]. The $j_{\mathrm{XR}}(r)$ curve has a first intense peak at $\simeq 1.9$ Å preceded by a shoulder at 1.5 Å, consistent with the experimental data reported in Refs. [10,11]. Indeed, in [10] it is seen that j_{XR} of a-$\mathrm{Si}_{1-x}\mathrm{C}_x$:H has a peak at $\simeq 1.9$ Å (1.85 Å) for $x = 0.75$ ($x = 0.35$) and a shoulder at 1.5 Å. Similar features at 1.9 and 1.5 Å are found in the DF $t(r) = 4\pi\rho_0 r[g(r) - 1]$ reported in [11] for evaporated a-$\mathrm{Si}_{1-x}\mathrm{C}_x$ ($x \simeq 0.5$). In x-ray scattering Si is weighted more than twice as much as C by its atomic $f_i(q)$ [e.g., $f_{\mathrm{Si}}(q)/f_{\mathrm{C}}(q) \simeq 2.3, 3.5, 2.6$ for $q = 0, 5, 10$ Å^{-1}, respectively], and therefore the intense peak of $g_{\mathrm{C\text{-}C}}$ (Fig. 1) appears only as a weak shoulder in j_{XR}. Furthermore, $g_{\mathrm{Si\text{-}Si}}$ is rather featureless and thus the Si-Si nearest-neighbor distance is not visible in j_{XR}. These two circumstances —large scattering from Si which masks the C-C correlations and disorder in the Si subsystem —conspire to give a rather prominent peak in j_{XR} at $\simeq 1.9$ Å, close to the Si-C distance in c-SiC. This has often been interpreted as a clear signature of chemical order in a-SiC, thus leading to a structural model rather different to that obtained in our simulation. Clearly the x-ray data alone cannot resolve the issue of chemical order nor can electron scattering (ES) experiments for which similar considerations apply [$f_{\mathrm{Si}}^{\mathrm{XR}}(q)/f_{\mathrm{C}}^{\mathrm{XR}}(q)$ is very similar to $f_{\mathrm{Si}}^{\mathrm{ES}}(q)/\ f_{\mathrm{C}}^{\mathrm{ES}}(q)$]. XAFS data [9,12], which use the Si adsorption edge, show a strong Si-C peak, suggesting again chemical order. However, even these results are in our opinion fully consistent with ours, since we expect XAFS backscattering interference to be dominated by the strong Si-C correlations, and the weaker and broader $g_{\mathrm{Si\text{-}Si}}$ to lead to a very blurred and hardly detectable feature.

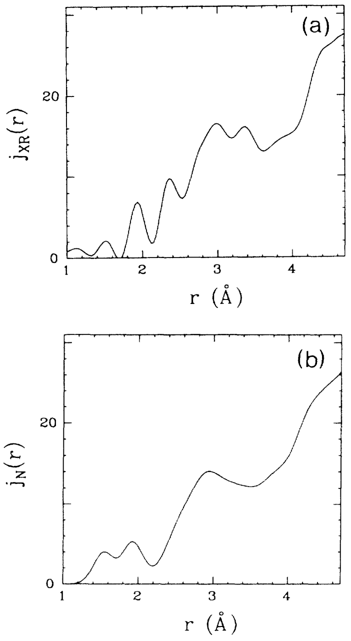

FIG. 2. Computed total distribution functions, to be compared with Fourier transforms of (a) x-ray [$j_{\mathrm{XR}}(r)$] and (b) neutron [$j_N(r)$] scattered intensities (see text). In (a) the bump at $r \lesssim 1.3$ Å is a spurious effect of the q-space cutoff used in our FT procedure (see Ref. [25]).

We suggest that neutron diffraction data are able to resolve this ambiguity. In fact neutron scattering can better resolve C-C correlations since the scattering cross sections of Si and C are more evenly balanced with a dominance of the C scattering. Figure 2(b) shows the distribution function $j_N(r)$ computed from

$$j_N(r) = \frac{\sum_{i,j} f_i^N f_j^N g_{i,j}(r)}{\sum_i (f_i^N)^2}, \tag{2}$$

where f_i^N are neutron scattering lengths [$f_{\mathrm{Si}}^N = 4.15$, $f_{\mathrm{C}}^N = 6.65$ fm] and $g_{i\text{-}j}$-computed PDF [27].

It is seen that $j_N(r)$ is quite different from $j_{\mathrm{XR}}(r)$, with its double peak at 1.5 and 1.9 Å, reflecting the presence of different kinds of bonds in the amorphous network. This is clearly at variance with the crystal.

The electronic properties of a-SiC have been analyzed in terms of the electronic density of states (EDOS) and its angular decomposition in s and p components (Fig. 3). The material is found to be a semiconductor, in agreement with experiment. The overall shape of our EDOS is also in close agreement with available photoemission spectra [22]. At the bottom of the valence band, whose width is slightly larger than that of c-SiC, predominantly C s states are found. They give rise to a double-peaked structure centered around -15 eV, which has been observed in photoemission spectra by Fang and Ley [6]. Another prominent feature is the disappearance of the ionicity gap at $\simeq -11$ eV which characterizes c-SiC EDOS. This is a manifestation of the randomness and lack of chemical order in a-SiC. The top of the valence band is clearly dominated by C and Si p states, whereas conduction-band states show a large homogeneity with respect to s and p character of both species.

In conclusion, we have presented MD simulations of a-SiC at stoichiometric composition which show that the system can be classified neither as chemically ordered since (40–45)% of the bonds are homonuclear nor as random since a high degree of short- to medium-range order exists. We expect that other amorphous alloys of chemi-

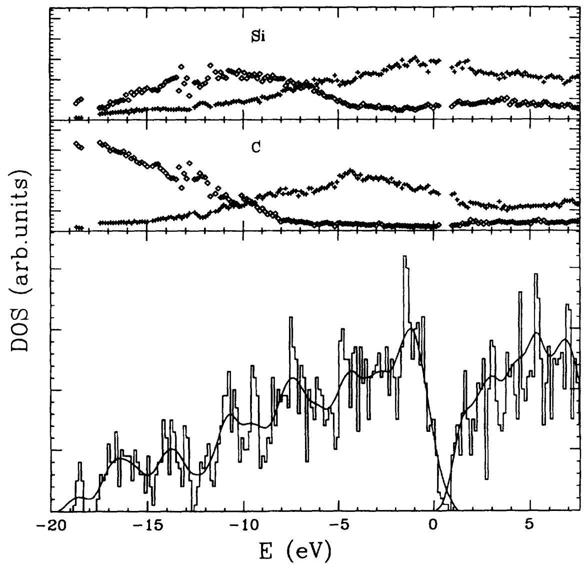

FIG. 3. The lower panel shows the electronic density of states (EDOS), computed as an average over 19 atomic configurations. (The solid line represents the convoluted data with $\Delta E \simeq 0.5$ eV.) The middle and upper panels show the angular decomposition of EDOS into s (diamonds) and p (crosses) components for C and Si, respectively. Spheres of radii 1.17 and 0.76 Å centered around Si and C have been chosen for the decomposition.

cally different elements will also display a similarly complex behavior. For all these systems reference to the perfect-crystal properties may be misleading. Only the access to atomic species correlations can determine the short-range order without ambiguities.

The computer resources have been provided by the IBM Research Laboratory in Zurich, by the Convention for Applications of Supercomputing for University and Research (CASPUR)-NIC project in Rome, and Consiglio Nazionale delle Ricerche through Progetto Finalizzato Sistemi Informatici e Calcolo Parallelo, Contract No. 90.00658.PF69. One of us (G.G.) acknowledges partial support from the Swiss National Science Foundation under Grant No. 21-31144.91.

---

[a] Present address: Institut Romand de Recherche Numérique en Physique des Matériaux (IRRMA), PHB Ecublens, 1015 Lausanne, Switzerland.

[b] Present address: Centre Européen de Calcul Atomique et Moléculaire (CECAM), Universitè Paris-Sud, 91405 Orsay, France.

[1] *Novel Refractory Semiconductors*, edited by D. Emin, T. L. Aselage, and C. Wood (Materials Research Society, Pittsburgh, 1987).

[2] *Amorphous and Crystalline Silicon Carbide and Related Materials*, edited by G. L. Harris and C. Y. Yang (Springer-Verlag, New York, 1989).

[3] P. C. Kelires, Europhys. Lett. **14**, 1 (1991).

[4] J. Robertson (to be published).

[5] M. Gorman and S. A. Solin, Solid State Commun. **15**, 761 (1974).

[6] L. C. Fang and L. Ley, Phys. Rev. B **40**, 3818 (1989).

[7] J. Tejeda, N. J. Shevchik, and M. Cardona, in *Proceedings of the Fifth International Conference on Amorphous and Liquid Semiconductors*, edited by J. Stuke and W. Brenig (Taylor and Francis, London, 1974), p. 557.

[8] W. Y. Lee, J. Appl. Phys. **51**, 3365 (1980).

[9] S. Pascarelli, F. Boscherini, S. Mobilio, and F. Evangelisti, Phys. Rev. B **45**, 1650 (1992).

[10] C. Meneghini *et al.*, J. Non-Cryst. Solids **137-138**, 75 (1991).

[11] A. Sproul, D. R. McKenzie, and D. J. H. Cockayne, Philos. Mag. B **54**, 113 (1986).

[12] A. E. Kaloyeros, R. B. Rizk, and J. B. Woodhouse, Phys. Rev. B **38**, 13099 (1988).

[13] O. Chauvet *et al.*, Mater. Sci. Forum **83**, 1201 (1992).

[14] R. Car and M. Parrinello, Phys. Rev. Lett. **55**, 2471 (1985).

[15] G. Galli *et al.*, Phys. Rev. Lett. **62**, 555 (1989); Phys. Rev. B **42**, 7470 (1990).

[16] I. Stich, R. Car, and M. Parrinello, Phys. Rev. B **44**, 11092 (1991).

[17] The pressure of our samples computed *a posteriori* indicates that the equilibrium volume of a-SiC is indeed very close to that of the crystal (about 2% smaller).

[18] G. B. Bachelet, D. R. Hamann, and M. Schlüter, Phys. Rev. B **26**, 4199 (1982); L. Kleinman and D. M. Bylander, Phys. Rev. Lett. **48**, 1425 (1982).

[19] The computed lattice constant of c-SiC in the diamond structure at zero T is found to be the same as the experimental one within 1%.

[20] In the simulation runs a time step equal to 4.0 a.u. was used and the fictitious mass parameter entering the Car-Parrinello equations of motion set at 300 a.u.

[21] A. H. Mahan *et al.*, J. Appl. Phys. **57**, 2717 (1984).

[22] Y. Katayama, K. Usami, and T. Shimada, Philos. Mag. B **43**, 283 (1981); Y. Katayama *et al.*, Physica (Amsterdam) **117B**, 947 (1983).

[23] M. A. Petrich, K. K. Gleason, and J. A. Reimer, Phys. Rev. B **36**, 9722 (1987).

[24] By varying the cutoff distance ($r^{\rm min}_{\rm Si\text{-}Si}$) from 2.5 to 2.6 Å, the value of $n_{\rm Si\text{-}Si}$ changes from 2.0 to 2.4; for $r^{\rm min}_{\rm Si\text{-}Si} = 2.5$ about 20% of the atoms are threefold coordinated, 10% fivefold coordinated, and the remaining fourfold coordinated. When $r^{\rm min}_{\rm Si\text{-}Si} = 2.6$ is chosen the number of threefold sites decreases to $\simeq 5\%$ and the proportion of fivefold sites rises to 30%.

[25] $j_{\rm XR}(r) = 4\pi r^2 \rho_0 g(r) = (r^2/2\pi^2)\int d\mathbf{q}[S(\mathbf{q}) - 1]\exp(i\mathbf{q}\cdot\mathbf{r})$. The FT has been performed with $q_{\rm max} = 20$ Å^{-1}, the same as the one used in XRD (Ref. [10]). We checked the accuracy of the FT procedure by comparing $g_{i\text{-}j}$ as computed from their definition (see Fig. 1) with those obtained from the FT of $S_{i,j}$. The peak positions and the relative intensities are found to be the same in both cases. However, small wiggles at $r \leq 1.3$ Å appear in the $g_{i\text{-}j}$ obtained from FT, due to the finite q-space cutoff.

[26] *International Tables of X-Ray Crystallography* (The Kynoch Press, Birmingham, 1962), pp. 201-209.

[27] Following J. H. Etherington *et al.* [J. Non-Cryst. Solids **48**, 265 (1982)], $j_N(r)$ has been convoluted with a resolution function corresponding to $q_{\rm max} = 20$ Å^{-1}, in order for the comparison with $j_{\rm XR}(r)$ to be completely consistent.